4.5mm below the dural surface; at tooth bar position 0.0mm). The retroviral vector solution was suctioned through the 31-gauge injection needle into a Hamilton microsyringe (Hamilton, Reno, NV) just before injection, and the trace viral solution on the surface of the needle was wiped out to avoid contamination. The needle was slowly placed into the target, and the vector solution was ejected at the rate of 1μl/min and was left steady for 5 minutes. Injection into the rat SN (AP, 5.3mm; ML, 2.4mm from bregma; DV, 7. mm, at tooth bar position −4.0 mm) was made using a similar procedure, but the injection volume was 2μl. To inject the vector into the area ventral to the midbrain aqueduct of mice (AP, −3.5mm; from bregma; DV, −3.5mm) and rats (AP, −5.3mm; from bregma; DV, 7.0mm from bregma), we angled the needle 15 degrees to the right to avoid the sinus. To compare the labeling with BrdU and retroviral vector, we injected some animals with BrdU (50mg/kg IP) just after retroviral injection.

Hemi-Parkinsonian Model

To evaluate the effect of dopamine deprivation on one section, we injected 1-methyl-4-phenylpyridinium salt into the left medial forebrain bundle of rats.[28] 1-Methyl-4-phenylpyridinium salt solution (5μg/μl × 2μl) was injected to the left (AP, −3.6mm; ML, 2.0mm; DV, −7.6mm from bregma) and 2μl saline was injected into the right medial forebrain bundle. A midbrain section of a hemi-parkinsonian macaque monkey[29,30] was stained for PSA. The monkey received slow infusion of MPTP (4mg) into the left caudate nucleus using an osmotic minipump and survived for 6 months after the infusion.

Brain Tissue Sections

Animals were deeply anesthetized with pentobarbital and perfused transcardially with PBS followed by perfusion with 10mM phosphate-buffered 4% formaldehyde solution (pH 7.4). Brains were postfixed in the same fixative for 2 days and allowed to sink in sucrose-PBS (30% sucrose in PBS containing 0.05% sodium azide). The brain tissue was frozen quickly in crushed dry-ice powder; coronal sections were sliced 25μm in thickness on a cryostat, and then stored in sucrose-PBS at 4°C until use.

The site of injection and expression of GFP was confirmed, and only brains showing the location of the injection were subjected to further studies. To identify the distribution of GFP expression, we stained every sixth section with anti-GFP antibody for light microscopy by streptavidin-biotin-peroxidase complex (ABC) and 3,3-diaminobenzidine (DAB). The remaining sections were subjected to double-immunofluorescence staining of TH and a glial marker and visualized using Cy3- and Cy5-conjugated secondary antibodies. At least 12 sections rostral and 12 caudal to the center of injection were stained and examined in each mouse.

Human brain tissue was obtained at Juntendo University Hospital, with the full consent of the family at the time of autopsy. The study protocol was approved by the Human Ethics Review Committee of Juntendo University School of Medicine. Midbrains of six patients with PD were studied, and those of six other neurological diseases (one with Alzheimer's disease, one myasthenia gravis, one muscular dystrophy, one vascular parkinsonism, and two cerebral hemorrhage) were included as the disease controls. The hemisphere of midbrain tissue was cut into blocks and fixed in buffered 4% formaldehyde solution for 2 days, and then moved to sucrose PBS until sink. The blocks were sectioned in the coronal plane (30μm in thickness) by a cryostat and further stored in sucrose PBS at 4°C. Because some sections were friable and easily torn off, human sections were incubated overnight in buffered 4% formaldehyde solution before starting immunostaining.

Double-Immunofluorescence Staining

The primary antibodies used in this study were anti-PSA (clone 12E3 mouse IgM)[24] at a working dilution of 1:500 to 1:2,000, goat anti-TH (1:2,000; Calbiochem, San Diego, CA), rabbit anti-ionized calcium-binding adaptor protein Iba-1 (1:2,000; Wako, Osaka, Japan),[31] rabbit anti-NG2 (1:200; Chemicon, Temecula, CA),[32] rabbit anti–glial fibrillary acidic protein (1:5,000; generous gift from Dr H. Akiyama, Psychiatric Research Institute of Tokyo, Tokyo, Japan), rabbit anti-Pi class glutathione-*S*-transferase–pi (1:10,000; MBL, Nagoya, Japan),[33] rabbit anti-GFP (1:1,000, Chemicon), mouse anti–rat cd11b (1:200; clone OX-42, Immunotech, Marseille, France), and rat anti-BrdU (1:400, clone BU1/75; OBT, Oxford, United Kingdom). Secondary antibodies of fluorescein isothiocyanate, Cy3, Cy5, or biotin-conjugated donkey IgG of minimal cross-species grade (Jackson Laboratories, West Grove, PA) were used at 1:500 dilution. Arexa-594–conjugated donkey anti–goat antibody (Molecular Probes, Eugene, OR) was used in some cases.

Fluorescent microscopic staining was performed as described previously[22,23] with minor modifications. PBS with 0.05% Triton X-100 (Sigma) was used throughout the incubation. Antibodies were diluted in blocking solution of 2% block ace protein solution (Yukijirusi, Sapporo, Japan) in PBS with 0.05% Triton X-100. All incubations were performed at the room temperature, except for anti-BrdU, which was incubated at 4°C. Free-floating sections stored in sucrose PBS were rinsed with PBS and treated with chilled methanol for 10 minutes at −20°C to improve permeability of the antibodies. Then, the sections were incubated in blocking solution for 1 hour followed by overnight incubation in the primary antibody diluted in the blocking solution at room temperature, rinsed in PBS with 0.05% Triton X-100, and then incubated in secondary antibodies. For BrdU staining, the sections were first incubated in 2N HCl (Wako) at 37°C for 30 minutes, neutralized with borate buffer (100mM, pH 8.5) for 10 minutes and PBS for 10 minutes, and incubated in anti-BrdU overnight at 4°C, then Cy3-conjugated anti–rat IgG for 1 hour. As HCl faded the green fluorescence of GFP, the BrdU-stained sections were further immunostained with anti-GFP and fluorescein isothiocyanate–conjugated anti–rabbit IgG.

Immunohistochemistry for Light Microscopy by Streptavidin-Biotin-Peroxidase Complex Method

For light microscopic examination, the tissue sections were stained with elite avidin-biotin complex kit (Vector Laboratories, Burlingame, CA), DAB tablet (Sigma), and Ni-Cl solution (Funakoshi, Tokyo, Japan), as described previous-

ly[26,34] with minor modifications. After treatment with the primary antibodies, the sections were incubated in biotin-conjugated secondary antibodies for 1 hour, and then treated with 3% H_2O_2 in 10% methanol for 10 minutes, treated streptavidin-biotin-peroxidase complex for 1 hour, and visualized with DAB solution for 10 minutes. To distinguish neuromelanin from immunostaining, we added 0.0008% NiCl to DAB solution in human midbrain sections.

Image Analysis and Quantification

The distribution of individual GFP-positive cells was plotted on a brain map. Objects with autofluorescence were discarded (Fig 1, I–M). GFP fluorescence possibly colocalized with TH was recorded on the map and was further confirmed by confocal microscopy (model LSM510 laser scanning microscope; Carl Zeiss Jena, Germany).

In the mouse study, double staining of TH was helpful to determine the location in SN. In human sections, the area with scattered neuromelanin was regarded as substantia nigra pars compacta (SNc), and the area between SNc and the cerebral peduncle was regarded as substantia nigra pars reticulata (SNr). PSA-stained human brain sections were evaluated by an observer blinded to the study protocol. The location of PSA-positive cells was plotted on a low-power photograph of the section. The density of DAB staining of PSA and TH of rat sections was determined using a proce-

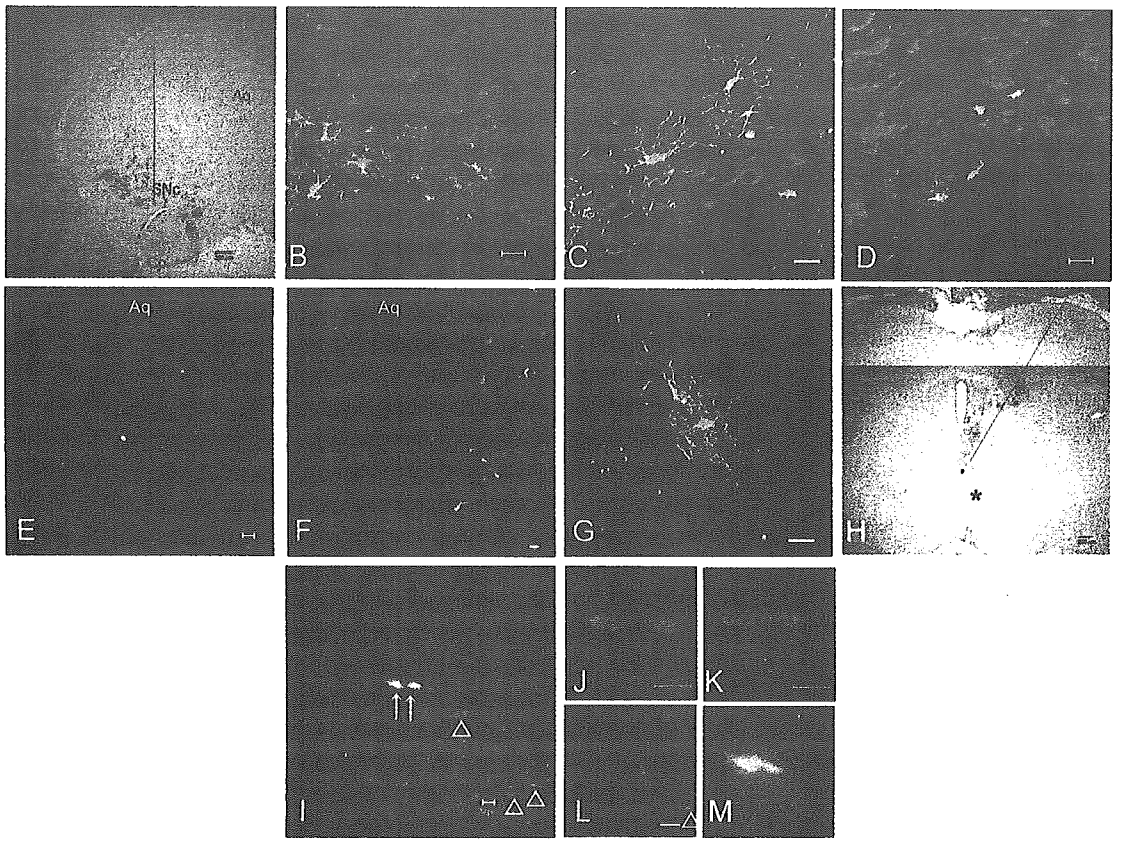

Fig 1. Retroviral green fluorescent protein (GFP) transduction in rodent substantia nigra and lack of colocalization with tyrosine hydroxylase (TH). (A) Low-power view of the injection site in a representative mouse 16 weeks after retroviral injection into the substantia nigra (Sal2d16w). Immunostained with anti-GFP followed by 3,3-diaminobenzidine. Several GFP-positive cells are present in the substantia nigra pars compacta (SNc), substantia nigra pars reticulata (SNr), and the cerebral peduncle. Aq = midbrain aqueduct; Cp = cerebral peduncle; Hi = hippocampus. (B) SN of an intact mouse 2 days after retroviral injection. GFP-positive cells (green) are present beside TH-positive cells (red). Examples of the substantia nigra of (C) a mouse A2d4w and a (D) rat-SN2w. (E) Injection site of an A7dAq4w mouse. Only one GFP-positive cell is present in this section. There are several TH-positive cells (red), but the GFP-cell is negative to TH. (F) Rat aqueduct area Rat-SN2d. (G) One GFP-positive cell (green) was present ventral to the midbrain aqueduct, but no such cells were present in the SN. (H) Low-power view of retroviral injection close to the midbrain aqueduct of a Rat-SN2d rat. An adjacent section to that shown in G and the approximate location of the cell in G is indicated with an asterisk. *(I–M) Example of a false-positive image found in the SN of a C7d4w mouse. (I) The TH-cell–like objects at the lateral end of the SNc indicated by* arrows *exhibit green and red fluorescence and appear yellow in the merged view. Three TH-positive cells on the right (red) are indicated by* arrowheads. *(J, K) Serial confocal images show that these two yellow figures in I are parts of one U-shaped object. (L, M) Nonlaser fluorescent view with red (L) and ultraviolet (UV) (M) filters of the same object in I. Blood vessels occasionally can cause autofluorescence and can be detected under UV excitation (M). (A, F, H)* Red lines *indicate the position of the injection needle. Bars = 20μm (B–G, I–M); 200μm (A, H).*

dure similar to that described previously[34] with LAS-1000 image analyzer (Fujifilm, Tokyo, Japan). The density unit of the corpus callosum of each section was subtracted as the background. Four coronal sections of the middle part of the rat SN (approximately 5.0, 5.18, 5.36 and 5.54mm posterior to bregma) were evaluated with densitometry.

Statistical Analysis

Cell colocalization data (Table 2) were analyzed by χ^2 test. Differences in the number of PSA-stained cells (see Fig 3) was analyzed with two-tailed U-test and density ratio of hemilesioned rat (see Fig 4) was analyzed by two-tailed *U*-test. $p < 0.05$ denoted a statistically significant difference.

Results

Retroviral Expression of Green Fluorescent Protein in Substantia Nigra

GFP was expressed in several cells around the injection site of SN of mice and rats (see Fig 1A–D). Expression of GFP was already evident 2 days after injection (see Fig 1B) and lasted for at least 16 weeks (see Fig 1A). The cell bodies of GFP-expressing cells were less than 10μm in diameter and had several fine processes. Typical TH-positive cells were larger and had bipolar shape. Coexpression of TH and GFP was not identified in mice treated with or without MPTP (see Tables 1 and 2). The results were similar in rats (see Fig 1D).

To study the possible migration of cells derived from neural stem/progenitor cells that are located in the periaqueductal area to SN, we injected the retroviral vector in an area adjacent to the midbrain aqueduct in mice (see Fig 1E) and rats (see Fig 1F, H). In mice, the number of labeled cells was small even at the center of the injection site (see Fig 1E), and no such cells were observed in the SN. They were more frequent in rats than in mice (see Fig 1F, H), but the distribution of GFP cells did not suggest their migration from the aqueduct area in a ventral direction. A few GFP-labeled cells were found in the ventral tegmental area (see Fig 1G), but none were identified in the SN.

Some autofluorescent objects were carefully discarded. The example shown in Figure 1I exhibits green and red fluorescence, but fine focusing on laser scanning microscope showed the image was two parts of one tubular structure (see Fig 1J, K). Examination under ultraviolet excitation light (see Fig 1M) was convenient for detecting autofluorescence. After fine analysis of morphology and autofluorescence, we could not identify TH-immunostained, GFP-expressing cells.

Cell Typing of Proliferating Cells in Substantia Nigra

These GFP-positive cells were characterized by staining with glial markers (Fig 2; see Table 2). GFP was colocalized with marker molecules of microglia Iba-1,[31] oligodendrocyte precursor NG2,[32] and oligodendrocyte (glutathione-*S*-transferase–pi, see Fig 2).[33] The number of GFP-labeled microglia was significantly larger than other protocols in mice of the acute MPTP treatment protocol 2 days before (see Table 2). This is consistent with our earlier observation of microglial activation 2 days after acute MPTP treatment.[26] The relative number of NG2 was reduced 2 days after MPTP and glutathione-*S*-transferase–pi–positive cells were reduced in all of MPTP treatments. Interestingly, no GFP-expressing cells colocalized with glial fibrillary acidic protein (see Fig 2C and Table 2).

To clarify whether the two labeling methods of DNA duplication, BrdU and retroviral vector, label the same cell population, we administered BrdU to some animals after retroviral injection into the SN. The nuclei of some GFP-labeled cells were BrdU-positive (see Fig 2F). The twin cells shown in Figure 2F are probably just after cell division. Both are retroviral vector- and BrdU-labeled proliferating cells, but the morphology of the cell was presented only by retroviral GFP expression.

Polysialic Acid Staining in Substantia Nigra of Humans, Monkeys, and Rodents

In the hippocampus of rodents and human, young neurons were immunostained with PSA (Fig 3A, C), as

Table 2. Number of GFP-Positive Cells Colocalized with Cell Typing Markers in the Ventral Tegmentum

Group	n	Iba-1 (microglia)	NG2 (oligoprecursor)	GFAP (astrocytes)	GST-pi (oligodendrocytes)	TH (DA neurons)
Sal2d4w	4	2/23	12/24	0/19	5/28	0/94
A2d4w	4	94/197[a]	16/127[a]	0/130	5/137[b]	0/591
A7d4w	4	8/85	31/56	0/52	1/51[b]	0/244
C7d4w	3	9/73	40/74	0/70	3/88[b]	0/305

The number of total GFP-positive cells detected in the ventral tegmentum (SNc, SNr, Cp, and VTA) is the denominator and the number of colocalized cells with one of the cell type markers is the numerator. Sections were double-immunostained with tyrosine hydroxylase and a glial marker, as shown in Figure 2. Two sections of each animal were stained, and the section closer to the center of retroviral injection was subjected to quantitative analysis. Each value represents the total cell number in sections of three to four animals.

[a]$p < 0.01$; [b]$p < 0.05$, compared with the other groups, by χ^2 test. Note the high colocalization of Iba-1 and low colocalization of NG2 in group A2d4w.

GFP = green fluorescent protein

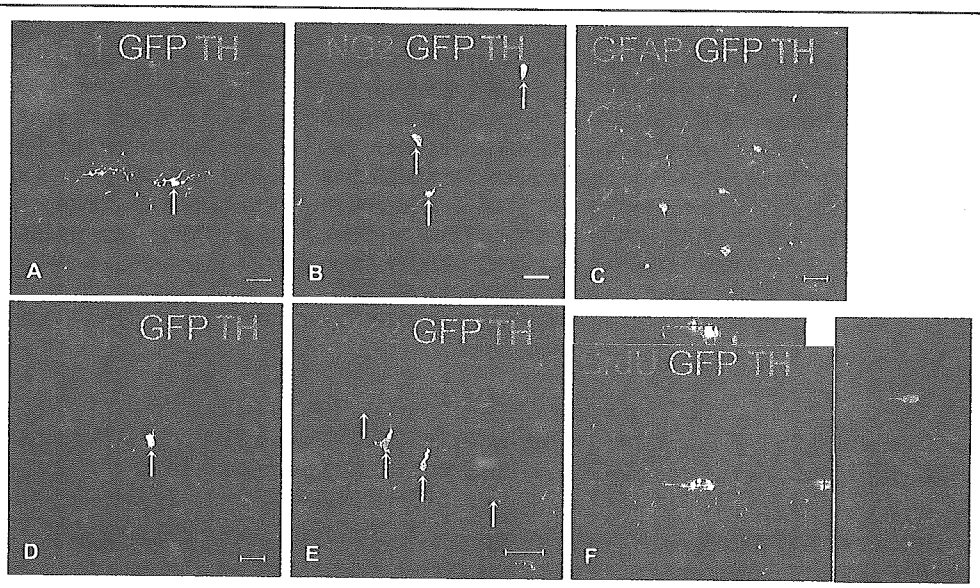

Fig 2. Colocalization of markers with green fluorescent protein (GFP)–expressing cells in the substantia nigra. Nigral sections of mice (A–D) and a rat (E) are immunostained with tyrosine hydroxylase (TH; blue) and a glial marker (red). (A) Iba-1 staining of an A2d4w mouse. Arrow *indicates a GFP-positive microglial cell expressing Iba-1 antigen. (B) NG2 staining of an A7d4w mouse.* Arrows *indicate GFP-positive cells covered with NG2 antigen on the cell surface. (C) Glial fibrillary acidic protein (GFAP) staining of an A2d4w mouse. No expression of GFAP is present among GFP-positive cells. (D) Glutathione-S-transferase–pi (GST-pi) staining of an A7d4w mouse.* Arrow *indicates GFP-positive oligodendrocyte expressing GST-pi. (E) OX-42 staining of a Rat-SN2d rat.* Arrows *indicate GFP-positive, microglia-expressing OX-42 antigen (CD11b) on the cell surface. (F) Comparison of two labeling methods of proliferating cells. These cells are positive for both retroviral transduction of GFP and bromodeoxyuridine (BrdU) incorporation to DNA and are probably just after cell division. Fine morphology of these cells is clearly drawn by GFP, whereas BrdU indicates only the nucleus. BrdU (50mg/kg intraperitoneally) was administered after local retroviral injection into the substantia nigra of a C7d4w mouse. This section was treated with HCl, followed by immunostaining with anti-BrdU and Cy3. The section was further immunostained with anti-GFP and fluorescein isothiocyanate, because HCl treatment reduced green fluorescence of GFP protein. Bars = 20μm.*

reported previously.[24,25] PSA-positive cells were found in the SN (see Fig 3B, D). Occasionally, PSA and TH double-positive cells were found in the SN of rats (see Fig 3B), although this was rare. There was considerable variance in the frequency of PSA-positive cells in human SN. There was no difference in the number of PSA-positive cells in the SNc (see Fig 3G) of patients with different conditions, but some PD sections contained many PSA-positive cells in the SNr (Fig 3H and Table 3). The cell numbers in PD tended to be different from those of disease control patients albeit insignificantly ($p < 0.06$, two-tailed t test). No such difference was noted in the SNc, which could be because of the dense PSA-positive fibers in the area just dorsal to the SNc. Similar results were noted in the monkey six months after MPTP infusion into the left caudate, with less TH staining and larger number of PSA-positive neurons in the ipsilateral SN (Fig 4).

Among the disease control cases, more than 100 PSA-positive melanized neurons were noted in the SNc of one cerebral hemorrhage case. PSA staining of melanized neurons was not often noted in the other brains. This interesting case indicates that human SNc neurons can express PSA in some conditions.

In addition to these 12 samples of free-floating sections, paraffin-embedded sections of human midbrain were also subjected to PSA immunostaining, but the staining was poor and further analysis was performed using only the floating sections. Staining for other intrinsic markers of neurogenesis was attempted, but double cortin was not clear in the SN and nestin gave intense staining of blood vessels but no staining of neurons in the SN, although it was evident in the hippocampus.

Human and monkey staining patterns of the SNr showed increased PSA-positive cells, but the results were not conclusive. The difference in the cell number was not significant, and the human samples were uneven about the cause of death and the midbrain level of the section.

We also examined the changes in PSA immunostaining after dopaminergic deprivation in rats. To evaluate the changes in hemilesioned rats by quantitative and objective measures, we compared the optic density of PSA immunostaining in the left and right SNr. The relative optic density of the lesioned SN to the intact SN was determined in the same section. In rats 2 months after 1-methyl-4-phenylpyridinium salt injec-

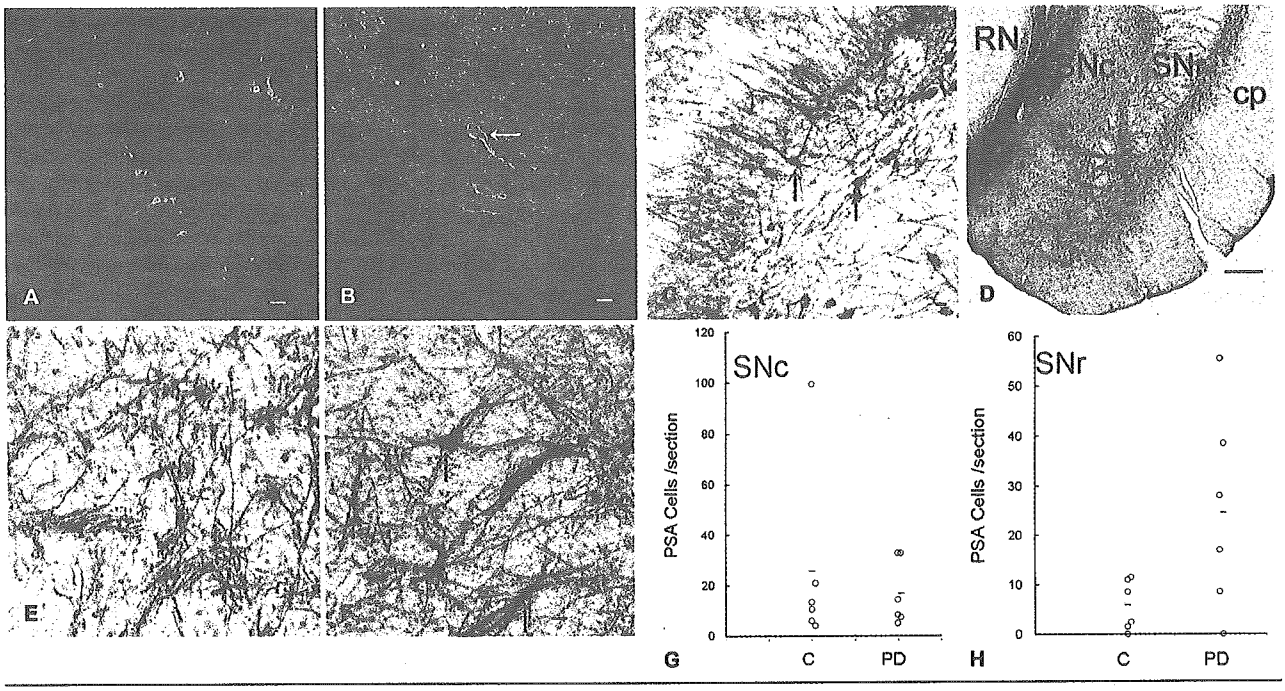

Fig 3. Polysialic acid (PSA)–positive cells in the substantia nigra. Sections of rats, a monkey, and humans are immunostained with monoclonal anti-PSA (clone 12E3). (A, B) Double immunofluorescence of PSA (green) and tyrosine hydroxylase (TH; red). (A) The subgranular zone of the rat hippocampal dentate gyrus is rich in PSA-positive young neurons. (B) The medial area of the substantia nigra of the rat. The surface of a substantia nigra pars compacta (SNc) TH-positive cell is covered with PSA (arrow). *(C, D) Immunostaining of human brain sections with anti-PSA and 3,3-diaminobenzidine. (C) Several cells of the subgranular zone of human hippocampus are PSA-positive* (arrows). *(D) Low-power view of human midbrain of a patient with Parkinson's disease. The area with melanin-containing neurons is regarded as SNc. PSA-positive fiber is dense in the area between SNc and red nucleus (RN). PSA-positive cells and fibers are scattered in substantia nigra pars reticulata (SNr). CP = cerebral peduncle. (E, F) PSA-positive cells in human substantia nigra* (arrows). *SNr of a control (E, muscular dystrophy) and Parkinson's disease (F) brain. (G, H) Number of PSA-positive cells in the SNc (G) and SNr (H) of human hemisphere sections. The average of duplicated counting of each sample by blinded observer is shown. Some nigral samples of Parkinson's disease showed the presence of large numbers of PSA-positive cells especially in the SNr, although the difference from the control brains was not statistically significant* ($p < 0.06$, *two-tailed* t *test). Scale bars = 20μm (A–C, E, F); 1mm (D). (C–F) Sections are counterstained with methyl green.*

tion into the left medial forebrain bundle, TH staining in the left SNc was reduced, whereas PSA staining in the SNr was increased (see Fig 4).

Discussion

Retroviral labeling of proliferating cells in rodents indicated lack of neurogenesis of TH-positive neurons from proliferative stem cells in the SN. In contrast, PSA-positive cells, candidates of newly differentiated young neurons, were present in the SN and increased in number after dopamine deprivation. Although we first intended to analyze dopaminergic neurons in the SNc, marked changes in PSA staining was detected in nondopaminergic neurons in SNr. Although PSA immunoreactivity is not conclusive evidence of neurogenesis,[35] the result suggests compensatory neuronal differentiation from mitotically silent cells.

Retrovirally Green Fluorescent Protein–Labeled Cells Did Not Differentiate into Dopaminergic Neurons

No GFP-positive cells after retroviral injection in the SN were found to express TH. This result is in agreement with some earlier studies[10,11,13] but not with one.[12] Double immunostaining in our study showed that the increased proliferative cells were mainly microglia, which was well in accordance with previous reports.[10,26] We also tried retroviral injection in close proximity to the midbrain aqueduct, but only a small number of cells were labeled and no migration to SN was observed. Because midbrain dopaminergic neurons originally migrate from the neural tube during development,[36] and TH-positive neurons distribute along the midline of the ventral tegmentum of adult animals,[37] it is quite an attractive idea that this area supplies dopaminergic neurons that ultimately migrate to reach the SN.[12] Local injection of a retroviral vector can give conclusive evidence of migration because it

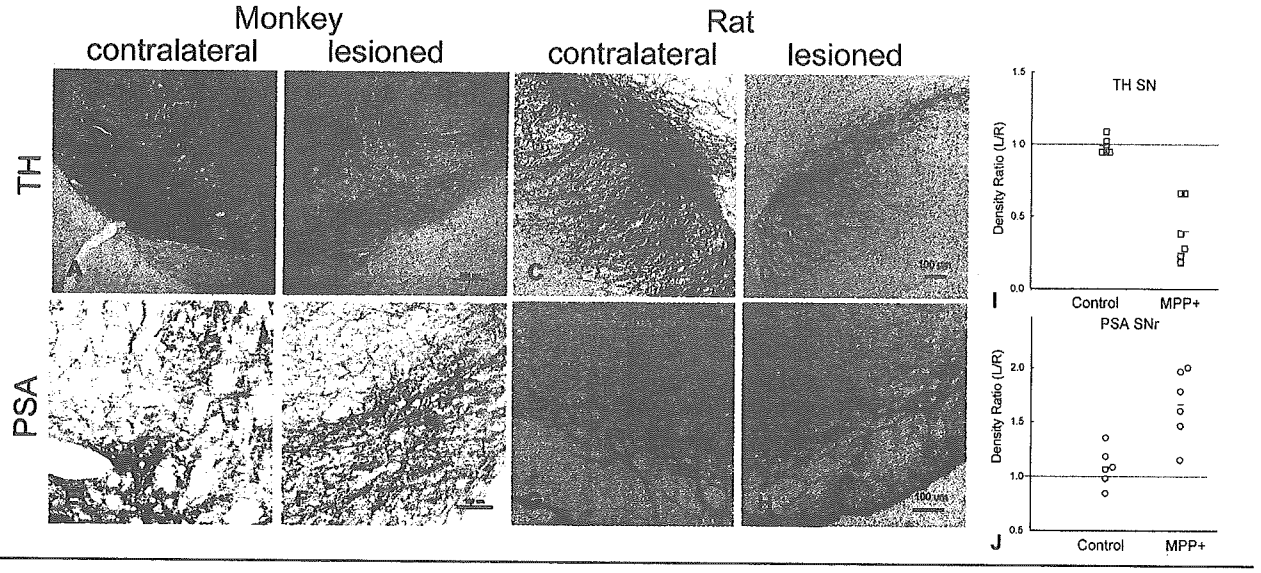

Fig 4. Changes in polysialic acid (PSA)–positive cells in hemilesioned animals. Substantia nigra of hemi-parkinsonian model monkey (A, B, E, F) and rat (C, D, G, H) showed reduced tyrosine hydroxylase (TH; A–D) and increased PSA (E–H) immunostaining. The substantia nigra of the monkey ipsilateral to 1-methyl-4-phenyl-1,2,3,6-tetrahydropyridine (Sigma, St. Louis, MO)–injected caudate (B, F) and that of the rat ipsilateral to 1-methyl-4-phenylpyridinium salt (MPP^+)–injected medial forebrain bundle (D, H) are shown side by side to their respective contralateral sides (A, C, E, G). (I, J) Six intact and six hemi-MPP^+ lesioned rats were subjected to densitometric analysis, and the results are expressed as the ratio of staining density of MPP^+-injected side to the saline-injected side. Each dot *represents one animal, and the* horizontal bars *indicate the average of the group. Marked reduction in TH* ($p < 0.01$) *and a slight increase in PSA* ($p < 0.01$) *immunostaining were detected in the MPP^+-treated side (two-tailed* t *test), whereas the ratio was almost even in the intact rats. Scale bars = 500μm (A, B); 100μm (C–H).*

can label the proliferating cells in a small area.[19,22] However, unlike the migration from subventricular zone (SVZ) to the olfactory bulb, the number of GFP-labeled cells beside the aqueduct was small, especially in mice. Because injection of the same retroviral solution into the dorsal striatum close to the lateral ventricle succeeded in labeling a large number of neuronal stem cells,[22] the small number noted in our study is not likely to be because of leakage of the viral solution into the aqueduct. Our preliminary study showed nestin, Ki67 immunostaining, and BrdU-positive nuclei after the current method of BrdU-administration was not evident around the midbrain aqueduct, whereas marked staining of them was noted in SVZ of the lateral ventricle (data not shown). These results suggest that the aqueduct area is not likely the source of new neurons in the adult midbrain.

Does Polysialic Acid in Substantia Nigra Suggest Neurogenesis?

Many cells in the SNr in PD midbrain were PSA-positive. Similar results were noted in the monkey and six rats after dopaminergic deprivation in the left hemisphere. In the hippocampus, PSA expresses on neurons under plastic changes of synapses and newly generated neurons.[24] In the midbrain, it is unclear whether PSA can be a marker of newly formed neurons.[35] Despite the negative results of retroviral labeling, it is possible that neurogenesis is present but undetectable by BrdU or retroviral vector. Neurogenesis in SVZ is well documented[38] and can be separated into three steps: proliferation, migration, and neuronal differentiation. BrdU and retroviral vector label DNA during its duplication. These methods have been effective in detecting neurogenesis in SVZ and hippocampus, but they are not direct markers of neuronal differentiation. Neural progenitor cells may not necessarily differentiate to neurons sequentially after cell proliferation. Actually, the cells start the final step of neuronal differentiation a few days after they reach the olfactory bulb.

Immature cells that can differentiate into neurons in vivo on transplantation into the hilar region of the hippocampus have been isolated from the adult rat midbrain.[11] It is unclear whether immature cells can differentiate into neurons and express PSA without cell division. In this study, most GFP-labeled cells were microglia and NG2-positive glial precursors (see Table 2), which can recover the multipotency and differentiate into neurons in certain environments.[39,40] These precursor cells may start neuronal differentiation without further proliferation when more neurons are required in the brain.

Regeneration of nigral neurons is still an attractive therapeutic target in PD. It is not appropriate to give a negative conclusion to this therapeutic possibility simply because the proliferative cells failed to differentiate

Table 3. Characteristics of Patients and Disease Controls

	Subject Age (yr)	Sex	Diagnosis	Duration of Illness	Yahr Stage	Dopa Treatment (yr)	PSA-Positive Cells[a]	
							SNc	SNr
Control								
	81	M	Cerebral infarction				6.0	0.0
	63	M	Myotonic muscular dystrophy				13.5	1.5
	57	F	Myasthenia gravis				21.0	2.5
	77	M	Cerebral hemorrhage				10.5	8.5
	92	M	Cerebral hemorrhage				99.5	11.0
	67	F	Alzheimer's disease				4.0	11.5
Mean	72.8						25.8	5.8
SD	12.9						36.6	5.1
PD								
	85	F	PD	13	5	13	7.5	0.0
	77	M	PD	7	4	7	5.0	8.5
	74	F	PD	8	4	8	8.5	17.0
	69	F	PD	9	4	7	33.0	28.0
	62	M	PD	13	3	13	33.0	38.5
	70	M	PD	16	4	16	14.5	55.5
Mean	72.8						16.9	24.6
SD	7.8						12.8[b]	20.4[c]

[a]The average of duplicate counting of each sample by blinded observer is shown. Data are aligned from top to bottom in the order of PSA cell number in SNr.
[b]$p < 0.05$; and [c]$p < 0.01$, significant difference of distribution, F-test.

PSA = polysialic acid; SNc = substantia nigra pars compacta; SNr = substantia nigra pars reticulata; SD = standard deviation; PD = Parkinson's disease.

into dopaminergic neurons. Nigrostriatal dopaminergic projection shows considerable recovery after MPTP treatment of animals, and a small number of TH-positive neurons appear in the SN after such treatment.[41–43] We speculate that the PSA-TH double-positive cells identified in this study represent newly generated dopaminergic neurons in the adult SN. In this regard, a recent study showed that dopaminergic agonists stimulate neurogenesis in SVZ.[43] It has been suggested that certain therapeutic agents currently in use, such as selegiline, ropinirole, and pramipexole, can slow the progress of the disease.[44,45] Further studies are warranted to examine the effects of these compounds on neurogenesis in the midbrain.

This work was supported by grants from the High Technology Research Center; the Ministry of Education, Culture, Sports, Science, and Technology, Japan (grant-in-aid for Scientific Research, B16390255, H.M.; S.M., Y.S.), Fujimoto Pharmaceuticals Corporation, (K.Y.), Ministry of Health, Labor and Welfare (S.M.), and the Tokyo Metropolitan Institute of Gerontology (S.M.).

We are grateful to Dr. H. Mori for providing human brain samples, Drs Y. Imai and S. Kohsaka for providing anti–Iba-1 antibody; Dr H. Akiyama for providing anti–glial fibrillary acidic protein antibody; H. Hayakawa for technical assistance; and Dr H. Imai for providing hemi-parkinsonian monkey brain sample. We thank Dr S. Fukuda for technical advice in confocal microscopy and for fruitful discussion.

References

1. Malberg JE, Eisch AJ, Nestler EJ, Duman RS. Chronic antidepressant treatment increases neurogenesis in adult rat hippocampus. J Neurosci 2000;20:9104–9110.
2. Banasr M, Hery M, Brezun JM, Daszuta A. Serotonin mediates oestrogen stimulation of cell proliferation in the adult dentate gyrus. Eur J Neurosci 2001;14:1417–1424.
3. Santarelli L, Saxe M, Gross C, et al. Requirement of hippocampal neurogenesis for the behavioral effects of antidepressants. Science 2003;301:805–809.
4. Armstrong RJ, Barker RA. Neurodegeneration: a failure of neuroregeneration? Lancet 2001;358:1174–1176.
5. Curtis MA, Penney EB, Pearson AG, et al. Increased cell proliferation and neurogenesis in the adult human Huntington's disease brain. Proc Natl Acad Sci U S A 2003;100:9023–9027.
6. Mikkonen M, Soininen H, Tapiola T, et al. Hippocampal plasticity in Alzheimer's disease: changes in highly polysialylated NCAM immunoreactivity in the hippocampal formation. Eur J Neurosci 1999;11:1754–1764.
7. Jin K, Peel AL, Mao XO, et al. Increased hippocampal neurogenesis in Alzheimer's disease. Proc Natl Acad Sci U S A 2004; 101:343–347.

8. Hirsch EC, Hunot S, Faucheux B, et al. Dopaminergic neurons degenerate by apoptosis in Parkinson's disease. Mov Disord 1999;14:383–385.
9. Olanow CW, Goetz CG, Kordower JH, et al. A double-blind controlled trial of bilateral fetal nigral transplantation in Parkinson's disease. Ann Neurol 2003;54:403–414.
10. Kay JN, Blum M. Differential response of ventral midbrain and striatal progenitor cells to lesions of the nigrostriatal dopaminergic projection. Dev Neurosci 2000;22:56–67.
11. Lie DC, Dziewczapolski G, Willhoite AR, et al. The adult substantia nigra contains progenitor cells with neurogenic potential. J Neurosci 2002;22:6639–6649.
12. Zhao M, Momma S, Delfani K, et al. Evidence for neurogenesis in the adult mammalian substantia nigra. Proc Natl Acad Sci U S A 2003;100:7925–7930.
13. Frielingsdorf H, Schwarz K, Brundin P, Mohapel P. No evidence for new dopaminergic neurons in the adult mammalian substantia nigra. Proc Natl Acad Sci U S A 2004;101: 10177–10182.
14. Nakatomi H, Kuriu T, Okabe S, et al. Regeneration of hippocampal pyramidal neurons after ischemic brain injury by recruitment of endogenous neural progenitors. Cell 2002;110: 429–441.
15. Zhu DY, Lau L, Liu SH, et al. Activation of cAMP-response-element-binding protein (CREB) after focal cerebral ischemia stimulates neurogenesis in the adult dentate gyrus. Proc Natl Acad Sci U S A 2004;101:9453–9457.
16. Kawai T, Takagi N, Miyake-Takagi K, et al. Characterization of BrdU-positive neurons induced by transient global ischemia in adult hippocampus. J Cereb Blood Flow Metab 2004;24: 548–555.
17. Rakic P. Adult neurogenesis in mammals: an identity crisis. J Neurosci 2002;22:614–618.
18. Gould E, Gross CG. Neurogenesis in adult mammals: some progress and problems. J Neurosci 2002;22:619–623.
19. Suzuki SO, Goldman JE. Multiple cell populations in the early postnatal subventricular zone take distinct migratory pathways: a dynamic study of glial and neuronal progenitor migration. J Neurosci 2003;23:4240–4250.
20. Kaneko S, Onodera M, Fujiki Y, et al. Simplified retroviral vector gcsap with murine stem cell virus long terminal repeat allows high and continued expression of enhanced green fluorescent protein by human hematopoietic progenitors engrafted in nonobese diabetic/severe combined immunodeficient mice. Hum Gene Ther 2001;12:35–44.
21. Suzuki A, Obi K, Urabe T, et al. Feasibility of ex vivo gene therapy for neurological disorders using the new retroviral vector GCDNsap packaged in the vesicular stomatitis virus G protein. J Neurochem 2002;82:953–960.
22. Yamada M, Onodera M, Mizuno Y, Mochizuki H. Neurogenesis in olfactory bulb identified by retroviral labeling in normal and 1-methyl-4-phenyl-1,2,3,6-tetrahydropyridine-treated adult mice. Neuroscience 2004;124:173–181.
23. Tanaka R, Yamashiro K, Mochizuki H, et al. Neurogenesis after transient global ischemia in the adult hippocampus visualized by improved retroviral vector. Stroke 2004;35:1454–1459.
24. Seki T, Arai Y. Highly polysialylated neural cell adhesion molecule (NCAM-H) is expressed by newly generated granule cells in the dentate gyrus of the adult rat. J Neurosci 1993;13: 2351–2358.
25. Fukuda S, Kato F, Tozuka Y, et al. Two distinct subpopulations of nestin-positive cells in adult mouse dentate gyrus. J Neurosci 2003;23:9357–9366.
26. Furuya T, Hayakawa H, Yamada M, et al. Caspase-11 mediates inflammatory dopaminergic cell death in the 1-methyl-4-phenyl-1,2,3,6-tetrahydropyridine mouse model of Parkinson's disease. J Neurosci 2004;24:1865–1872.
27. Przedborski S, Jackson-Lewis V, Naini AB, et al. The parkinsonian toxin 1-methyl-4-phenyl-1,2,3,6-tetrahydropyridine (MPTP): a technical review of its utility and safety. J Neurochem 2001;76:1265–1274.
28. Altar CA, Heikkila RE, Manzino L, Marien MR. 1-Methyl-4-phenylpyridine (MPP+): regional dopamine neuron uptake, toxicity, and novel rotational behavior following dopamine receptor proliferation. Eur J Pharmacol 1986;131:199–209.
29. Imai H, Nakamura T, Endo K, Narabayashi H. Hemiparkinsonism in monkeys after unilateral caudate nucleus infusion of 1-methyl-4-phenyl-1,2,3,6-tetrahydropyridine (MPTP): behavior and histology. Brain Res 1988;474:327–332.
30. Mochizuki H, Imai H, Endo K, et al. Iron accumulation in the substantia nigra of 1-methyl-4-phenyl-1,2,3,6- tetrahydropyridine (MPTP)-induced hemiparkinsonian monkeys. Neurosci Lett 1994;168:251–253.
31. Ito D, Imai Y, Ohsawa K, et al. Microglia-specific localisation of a novel calcium binding protein, Iba1. Brain Res Mol Brain Res 1998;57:1–9.
32. Dawson MR, Levine JM, Reynolds R. NG2-expressing cells in the central nervous system: are they oligodendroglial progenitors? J Neurosci Res 2000;61:471–479.
33. Cammer W, Zhang H. Localization of Pi class glutathione-S-transferase in the forebrains of neonatal and young rats: evidence for separation of astrocytic and oligodendrocytic lineages. J Comp Neurol 1992;321:40–45.
34. Yoshimi K, Iwata N, Takeda M, et al. Ischaemia-induced change in clathrin preceding delayed neuronal death. Neuroreport 1995;6:453–456.
35. Nomura T, Yabe T, Rosenthal ES, Krzan M, Schwartz JP. PSA-NCAM distinguishes reactive astrocytes in 6-OHDA-lesioned substantia nigra from those in the striatal terminal fields. J Neurosci Res 2000;6:588–596.
36. Kawano H, Ohyama K, Kawamura K, Nagatsu I. Migration of dopaminergic neurons in the embryonic mesencephalon of mice. Brain Res Dev Brain Res 1995;86:101–113.
37. Hokfelt-T, Martensson-R, Bjorklund-A, et al. Distributional maps of tyrosine-hydroxylase-immunoreactive neurons in the rat brain. Handbook of chemical neuroanatomy. Vol 2. New York: Elsevier, 1984:277.
38. Alvarez-Buylla A, Garcia-Verdugo JM. Neurogenesis in adult subventricular zone. J Neurosci 2002;22:629–634.
39. Belachew S, Chittajallu R, Aguirre AA, et al. Postnatal NG2 proteoglycan-expressing progenitor cells are intrinsically multipotent and generate functional neurons. J Cell Biol 2003;161: 169–186.
40. Yokoyama A, Yang L, Itoh S, et al. Microglia, a potential source of neurons, astrocytes, and oligodendrocytes. Glia 2004; 45:96–104.
41. Jackson-Lewis V, Jakowec M, Burke RE, Przedborski S. Time course and morphology of dopaminergic neuronal death caused by the neurotoxin 1-methyl-4-phenyl-1,2,3,6-tetrahydropyridine. Neurodegeneration 1995;4:257–269.
42. Ho A, Blum M. Induction of interleukin-1 associated with compensatory dopaminergic sprouting in the denervated striatum of young mice: model of aging and neurodegenerative disease. J Neurosci 1998;18:5614–5629.
43. Hoglinger GU, Rizk P, Muriel MP, et al. Dopamine depletion impairs precursor cell proliferation in Parkinson disease. Nat Neurosci 2004;7:726–735.
44. Marek K, Jennings D, Seibyl J. Do dopamine agonists or levodopa modify Parkinson's disease progression? Eur J Neurol 2002;9(suppl 3):15–22.
45. Stocchi F, Olanow CW. Neuroprotection in Parkinson's disease: clinical trials. Ann Neurol 2003;53(suppl 3):S87–S97.

ated. Approximately 1 day after the initiation of the therapy, the patient's INO had almost disappeared, but marked unilateral convergence palsy and subtle adduction palsy in his left eye remained (fig. 2). He was discharged 4 days after admission, at which time the intravenous antiplatelet therapy was changed to oral administration of aspirin at 100 mg/day. Approximately 1 month after onset, the patient's neuro-ophthalmological abnormalities had completely disappeared.

Discussion

Our patient showed unilateral INO together with convergence palsy; the former improved within 24 h with antiplatelet therapy, while the latter remained for approximately 1 month. Left INO might have been caused by transient ischemia influencing the left medial longitudinal fasciculus (MLF), whereas left convergence palsy could have been the result of a tiny midbrain infarction which seemed to be out of the MLF on MRI scans. We believe that diffusion-weighted imaging failed to reveal the infarction because its spatial resolution was insufficient to depict this tiny lesion.

Recently, Kim [1] has reported the clinical profiles of 30 patients who had INO as an isolated or predominant symptom of brainstem infarction [2]. In his report, 12 of the 30 patients had both convergence palsy and INO, and furthermore, 4 patients had those without exotropia of the contralateral eye. All of these 4 patients without exotropia had lesions in the midbrain or the isthmus, whereas some of the patients who had both convergence palsy and INO together with contralateral exotropia had lesions in the pons. Because convergence palsy with contralateral exotropia may cause insufficient vergence effort, it is suggested that the responsible lesions for convergence palsy in patients with INO are located in the midbrain or the isthmus, where the MLF may be part of the oculomotor complex. However, the lesion in the present patient seemed to be out of the MLF/oculomotor complex.

In both monkeys and humans, the cerebral cortical convergence center (Brodmann's areas 8, 18, 19 and 22) [5–8] projects into the bilateral oculomotor nuclei (medial rectus motoneurons), and primarily into the ipsilateral ones [5, 8]. This convergence pathway shows partial decussation in the thalamotectal areas before it reaches the oculomotor nucleus in the midbrain [2]. Neurons involved in vergence control (convergence neurons) have been found at 1–2 mm dorsal and dorsolateral to the oculomotor nucleus [3–5], and they receive bilateral input from the cortical convergence center. Convergence neurons project into the medial rectus motoneurons, which may have a selective function in vergence and which are located in the dorsomedial and rostral portions of the oculomotor nuclei [3].

The tiny dorsal midbrain infarction in our patient, which probably caused his convergence palsy, may not have been located on the MLF but on the convergence pathway. This lesion may have blocked the convergence pathway just before it reached the ipsilateral oculomotor nucleus. The present case provides important data for a greater understanding of the convergence pathway in humans.

References

1 Kim JS: Internuclear ophthalmoplegia as an isolated or predominant symptom of brainstem infarction. Neurology 2004;62:1491–1496.
2 Lindner K, Hitzenberger P, Drlicek M, Grisold W: Dissociated unilateral convergence paralysis in a patient with thalamotectal haemorrhage. J Neurol Neurosurg Psychiatry 1992;55:731–733.
3 Leigh RJ, Zee DS: Vergence eye movements; in Leigh RJ, Zee DS (eds): The Neurology of Eye Movements, ed 3. New York, Oxford University Press, 1999, pp 286–318.
4 Mays LE: Neural control of vergence eye movements: convergence and divergence neurons in midbrain. J Neurophysiol 1984;51:1091–1108.
5 Judge SJ, Cumming G: Neurons in the monkey midbrain with activity related to vergence eye movement and accommodation. J Neurophysiol 1986;55:915–930.
6 Warwick R: The so-called nucleus of convergence. Brain 1955;78:92–114.
7 Jampel RS: Presentation of the near response on the cerebral cortex of the macaque. Am J Ophthalmol 1959;48:573–582.
8 Ohtsuka K, Maekawa H, Takeda M, Ueda N, Chiba S: Accommodation and convergence insufficiency with left middle cerebral artery occlusion. Am J Ophthalmol 1988;106:60–64.

Shoichi Ito, MD, Department of Neurology
Graduate School of Medicine, Chiba University
1-8-1 Inohana, Chuo-ku, Chiba, 260-8670 (Japan)
Tel. +81 43 226 2126, Fax +81 43 226 2160
E-Mail sito@faculty.chiba-u.jp

Eur Neurol 2005;54:164–166
DOI: 10.1159/000090108

Man-in-the-Barrel Syndrome Caused by Bilateral Intratumoral Hemorrhage

Shunsuke Kobayashi[a], *Hirokazu Taniguchi*[b], *Shigeo Murayama*[a,c], *Masaki Sakurai*[a,d], *Ichiro Kanazawa*[a,e]

[a]Department of Neurology, Division of Neuroscience, Graduate School of Medicine, University of Tokyo; [b]National Cancer Center Hospital, Diagnostic Pathology Division; [c]Department of Neuropathology, Tokyo Metropolitan Institute of Gerontology; [d]Department of Physiology, Teikyo University School of Medicine, and [e]National Center of Neurology and Psychiatry, Tokyo, Japan

Introduction

Motor areas corresponding to the bilateral lower extremities lie adjacent on the medial side of the primary motor areas. Diplegia of the lower extremities is known to be caused by mid-sagittal lesions, e.g. due to compression by meningioma. In contrast, the bilateral brachial motor areas lay apart from each other on the lateral side of the primary motor areas. Brachial diplegia produced by a focal lesion in the cerebral cortex therefore is rare. Brachial diplegia, however, is known to be caused by systemic hypotension as a result of border zone infarctions in the cerebral cortex. The term 'man-in-the-barrel syndrome' (MIB) was coined by J.P. Mohr to describe brachial diplegia with intact motor function of the legs because such patients look as if they were restricted in the barrel [1]. To our knowledge, this article presents the first case of MIB syndrome caused by intratumoral hemorrhage of symmetrical tumors in the bilateral central gyri.

Case Report

A 72-year-old man with no history of malignancy was evaluated for progressive fatigue and arm weakness on both sides. He was a long-term smoker. On examination by a neurologist, weakness was detected bilaterally on the upper extremities, but there was no other detectable dysfunction of facial, extraocular, bulbar and lower extremity muscles. Bilateral arm weakness continued to progress over the next several days, and he was transferred to our hospital. On admission, his blood pressure was 150/80 mm Hg, and his pulse rate 110/min. His temperature was 36.4°C. The cervical lymph nodes and supraclavicular lymph nodes were palpable bilaterally. Rhonchi were heard in the right upper lung field. Neurological examination revealed an alert, fully oriented man with pupils equally reactive to light. He had ophthalmoplegia, mild bilateral facial palsy, mild pseudobulbar palsy, and severe paresis of the bilateral upper extremities. Leg motor function was intact on admission, but moderate paresis of the left leg progressed in the following days. Deep tendon reflexes were increased bilaterally. The left planter response was extensor. His sensory system was found to be intact. Blood cell counts were normal, except for elevated white-cell count (13,500/mm^3). There was no evidence of disseminated intravascular coagulation. A chest radiograph showed an opaque region in the right upper lung field. Computed tomographic (CT) scanning of the brain revealed high signal areas in the bilateral parietal regions. Brain magnetic resonance imaging (MRI) showed symmetrical round lesions bilaterally at the central gyri (fig. 1a, b). These lesions had fluid-fluid levels, the upper layer giving a low signal on the T1-weighted image (T1WI; fig. 1a) and a high signal on the T2-weighted image (T2WI; fig. 1b). The lower layer was iso-signal on T1WI and low signal on T2WI. The surrounding wall showed enhancement by Gd-DTPA (fig. 1a). Under the diagnosis of metastatic brain tumors of lung origin, whole brain radiation was started. Follow-up CT scans showed no change in tumor size or signs of brain herniation. Consciousness disturbance progressed gradually, and radiation therapy was stopped at 9 Gy in total. He died of cachexia 27 days after the onset of symptoms. Autopsy results showed pleomorphic carcinoma of the lung that had metastasized to the systemic lymph nodes, liver, spleen, stomach, colon, and brain. Most metastasis sites showed intratumoral hemorrhage. The bilateral precentral gyri were filled with hematoma (fig. 2). There were two other metastatic tumors in the bilateral ventral occipital lobes, each was 5 mm in diameter. No evidence of lesion was found elsewhere in the brain, most notably the brainstem was intact.

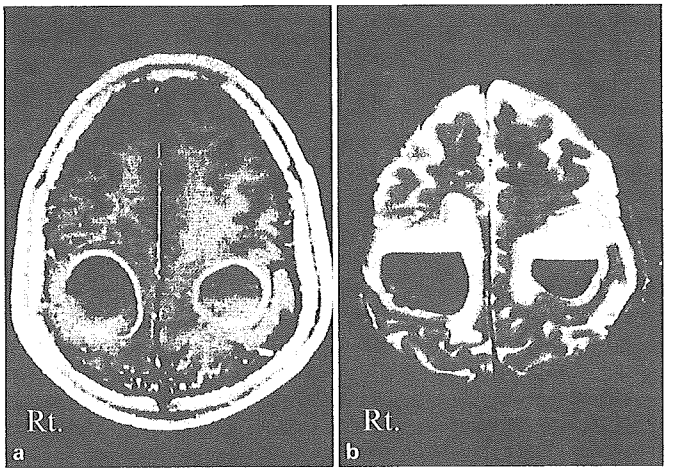

Fig. 1. Brain MRI one week after the onset of brachial diplegia. The rim of the symmetrical round cyctic lesions was enhanced by Gd-DTPA (**a** T1-weighted image). **b** T2-weighted image showed niveau formation inside the cystic lesions.

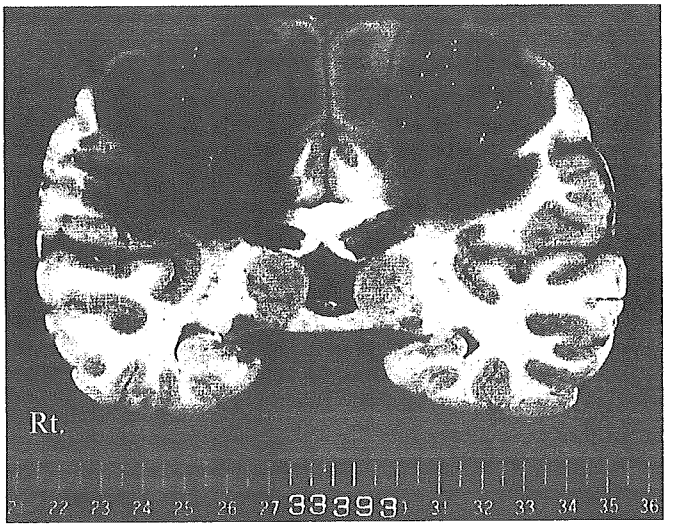

Fig. 2. A coronal section of the brain through the lateral geniculate bodies. Bilateral intracerebral hemorrhage was observed in the subcortical white matter of the precentral gyri.

Discussion

The term MIB was proposed to describe the brachial diplegia due to hypoperfusion in the cerebral cortex [1]. In some reports, brachial diplegia produced by a lesion in the brainstem or spinal cord is also called MIB. Strictly speaking, however, MIB should be used only for brachial diplegia caused by a supratentorial lesion(s) [2]. 'Cruciate paralysis' has been proposed to define brachial diplegia produced by a lesion in the pyramidal decussation [3], and 'central spinal cord syndrome' for the brachial dominant paresis produced by a cervical spinal cord lesion [4]. In our case, initial manifestation was pure brachial diplegia, which was produced by tumors in the bilateral central gyri. In the later course, our patient showed symptoms not characteristic of MIB, i.e. facial palsy, pseudobulbar palsy, ophthalmoplegia, and unilateral leg paresis. They can be explained by further involvement of cortical motor areas (face motor area, the frontal eye field, and leg motor area, which are lateral, rostral, and medial to the brachial motor area, respectively) or their descending projection fibers, probably due to extension of tumors and surrounding edema. The fact that the right-side tumor was closer to the medial wall than the left-side tumor (fig. 2) is consistent with the asymmetric symptom of the left leg weakness.

MIB is usually a consequence of watershed infarctions in the brachial motor areas located in border zones between the anterior

and middle cerebral artery territories. Typically, it occurs after cardiopulmonary arrest, hypovolemic shock, an overdose of narcotics, hypotension after myocardial infarction, or airway occlusion [1, 5]. In a prospective study of 28 patients who had systemic hypotension, 9 had MIB [6]. Moore and Humphrey reported a patient with metastatic brain lymphoma who developed MIB after systemic hypotension during bronchoscopy [7]. In their case, the tumors may have increased the susceptibility of the surrounding tissue to ischemia due to mechanical compression and tumor-surrounding edema, but the main cause of MIB appears to be border zone infarction. In our patient, however, intratumoral hemorrhage was the main cause of MIB. The reason why tumor metastasized symmetrically around bilateral central gyri is unclear. Possibly carcinoma cells had particular affinity for this area [8]. Another possibility is that tumor metastases may also prefer the watershed areas; it was suggested that tumoral microemboli tend to lodge in the capillaries of the distal parts of the superficial arteries [9].

Brachial diplegia is a rare and unique symptom. Its origin, however, may vary, being the cerebral cortex, brainstem, spinal cord, or peripheral nerve. Although most MIB cases are caused by infarcts in border zones between the anterior and middle cerebral artery territories, nonischemic causes, such as tumor and hemorrhage, may also cause MIB.

Acknowledgement

We thank Dr. Martin O'Neill for his comments on our manuscript.

References

1 Mohr JP: Distal field infarction. Neurology 1969;12:279.
2 Georgiadis D, Schulte-Mattler WJ: Cruciate paralysis or man-in-the-barrel syndrome? Report of a case of brachial diplegia. Acta Neurol Scand 2002; 105:337–340.
3 Bell HS: Paralysis of both arms from injury of the upper portion of the pyramidal decussation: 'cruciate paralysis'. J Neurosurg 1970;33:376–380.
4 Schneider RC, Cherry GL, Pantek HE: The syndrome of acute central cervical spinal cord injury. J Neurosurg 1954;11:564–577.
5 Sage JI, Van Uitert RL: Man-in-the-barrel syndrome. Neurology 1986;36: 1102–1103.
6 Sage JI: 'Man in the barrel syndrome' after cerebral hypoperfusion: clinical description, incidence and prognosis. Ann Neurol 1983;14:131.
7 Moore AP, Humphrey DM: Man-in-the-barrel syndrome caused by cerebral metastases. Neurology 1989;39:1134–1135.
8 Yeatman TJ, Nicolson GL: Molecular basis of tumor progression: mechanism of organ-specific tumor metastasis. Semin Surg Oncol 1993;9:256–263.
9 Delattre JY, Krol G, Thaler HT, Posner JB: Distribution of brain metastases. Arch Neurol 1988;45:741–744.

Shunsuke Kobayashi, MD, PhD
Department of Anatomy, University of Cambridge
Downing Street, Cambridge, CB2 3DY (UK)
Tel. +44 1223 339544, Fax +44 1223 333786
E-Mail skoba-tky@umin.ac.jp

Eur Neurol 2005;54:166–170
DOI: 10.1159/000090109

Improvement of Obsessive-Compulsive Disorder following Left Putaminal Hemorrhage

T. Fujii[a], *Y. Otsuka*[b], *K. Suzuki*[a], *K. Endo*[a], *A. Yamadori*[c]

[a]Department of Behavioral Neurology and Cognitive Neuroscience, Tohoku University Graduate School of Medicine, Sendai, [b]Department of Psychiatry, Asahi Chuo Hospital, Chiba, and [c]Department of Humanities and Sciences, Kobe Gakuin University, Kobe, Japan

Introduction

Obsessive-compulsive disorder (OCD) is characterized by recurrent obsessions or compulsions that are severe enough to be time consuming or cause marked distress or significant impairment. The patient recognizes that the obsessions or compulsions are excessive or unreasonable [1]. There have been several case studies of patients with OCD-like disorders following brain damage [2–11]. Also, there have been several studies using PET or SPECT and proposals concerning the relationship between OCD and dysfunction of the prefrontal-subcortical circuits [12–15]. However, it is still unknown whether OCD is determined by dysfunction of a particular link between specific brain regions within the prefrontal-subcortical loop. We herein describe a patient who showed improvement of long-standing OCD after the onset of left putaminal hemorrhage. To our knowledge, this is the first report of a patient who showed an improvement of OCD after brain damage and it provides evidence that the lenticular nuclei have modulating influences on the manifestation of OCD.

Case Report

The patient was a 58-year-old, right-handed man with a 21st-grade education. From the age of 43, he had suffered OCD characterized by contamination concerns with washing compulsions, which he realized were excessive and unreasonable. From the age of 55, he had been an outpatient of the department of psychiatry in a municipal hospital. For 2 years, several kinds of antidepressants, antipsychotic and antianxiety drugs were prescribed for his OCD. However, these drugs were not effective and the psychiatrist stopped prescribing these drugs. The patient also had hypertension from the age of 50, which was not treated. The patient had sudden onset of right hemiparesis and aphasia during washing compulsions, and was admitted to the department of neurosurgery of the municipal hospital. Brain CT on the day of onset showed intracranial hemorrhage centered on the left putamen probably due to long-standing untreated hypertension. Approximately 1 week after the stroke onset, his washing compulsions reappeared to a lesser degree. One month after hemorrhage, the patient was admitted to the Tohoku University Hospital for assessment and rehabilitation of right hemiparesis and aphasia.

On admission, the patient was alert and oriented to time and place. He was cooperative and not apathetic. General physical examination was unremarkable. The confrontation test revealed a defect in the visual field of the rightmost side. Both pupils were equal and round and reacted to light. Eye movement was full, with

神経Behçet病の病理

Pathology of neuro-Behçet disease

村山繁雄
Shigeo Murayama
東京都老人総合研究所老年病ゲノム(神経病理)

◎Behçet病は原因不明の炎症性疾患で，神経系では中脳・視床が高頻度に障害され，脳神経麻痺・錐体路徴候・進行性認知症(痴呆)が主症状となる．神経病理学的には，髄膜脳炎のかたちをとる．髄膜炎はくも膜下腔の小血管周囲のリンパ球浸潤よりなる．脳実質炎は，一部脱髄の要素をもった虚血性病変が主体であり，微小出血を伴うことが多く，病変部は進行性の萎縮をきたす．剖検時，小血管周囲を中心とするリンパ球浸潤と浮腫よりなる進行性病変を局所性に認めることが一般的で，慢性進行性の経過を示す．大動脈炎様病態をとる場合もある．HLA-B51が高頻度に認められるが，このHLA型の神経病理学的所見への影響ははっきりしない．

Key word：血管炎，梗塞，出血，脱髄，脳幹脳炎

神経Behçet病の基本病理は，髄膜炎と脳実質炎であり，視床・中脳が高頻度に侵される．脳幹脳炎としての脳神経麻痺と錐体路徴候，テント上病変によると考えられる進行性の認知症(痴呆)が特徴的である．

組織学的に，くも膜下腔の血管周囲にリンパ球・形質細胞の浸潤を認めるが，慢性例では線維化のみがめだつ場合もある．脳実質炎症は，最小動脈から毛細血管・小静脈に至る小血管周囲のリンパ球浸潤であり，微細な小軟化・壊死巣の融合のかたちをとり，不完全な脱髄所見の様相を一般に呈する[1]．鑑別としてヘルペス脳炎，サルコイドーシス，多発性硬化症などがあげられる．Behçet病は不全型が多いため，剖検しても診断が確定しないことがありうる．

以下に，自験例3例を呈示する．症例1は急性散在性脱髄性脳炎(ADEM)様の病像を呈した例，症例2は慢性脳炎様経過をとった例，症例3は頸部動脈の血管炎を併発したと考えられる例で，いずれも類似報告例がある．Behçet病に好発とされるHLA-B51はどの例でも認められていない．

症例呈示

1．症例1[2]

63歳ごろより口腔内や舌に小潰瘍が頻発．65歳ごろより両下肢に有痛性の結節性紅斑が頻発，陰嚢に潰瘍ができるようになった．68歳時，頭痛と歩行時のふらつきを認めるようになり，物静かな性格から大声で多弁となった．1カ月後に構音障害も出現し，近医より紹介入院，微熱，上記所見に加え，上肢毛嚢炎を認めた．神経学的に，多幸的児戯的性格変化，改訂型長谷川式簡易痴呆スケール24/30, IQ73点(WAIS-R VIQ77, PIQ74)，左視力低下(右1.0，左0.2)，眼科的に左黄斑部変性を指摘された．また，下顎反射は軽度亢進，右軽度不全麻痺，四肢深部反射すべて亢進，右Babinski徴候陽性を認めた．CT上左視床から橋にかけて内部に高信号域を伴う低信号域が広がっていた．MRI T1強調造影画像では左橋上部中央に輪状造影効果を認め，さらに左大脳脚に造影効果を認めた(図1)．T2強調画像では同レベルの橋は広範な高輝度を示し，中央には低信号域が認められた．血液検査で，白血球11,500/mm^3, CRP4.3 mg/dl, 赤沈27 mm/hr, 髄液蛋白41.6 mg/dl, 細胞数38/mm^3 (L：N＝88.3：12.7)，糖53 mg/dl, IL-6 119 pg/ml

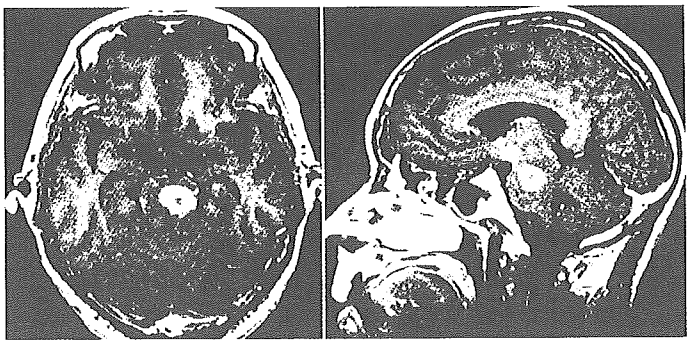

図 1　症例1，発症時のMRI[1)]
Ring enhance を伴う．

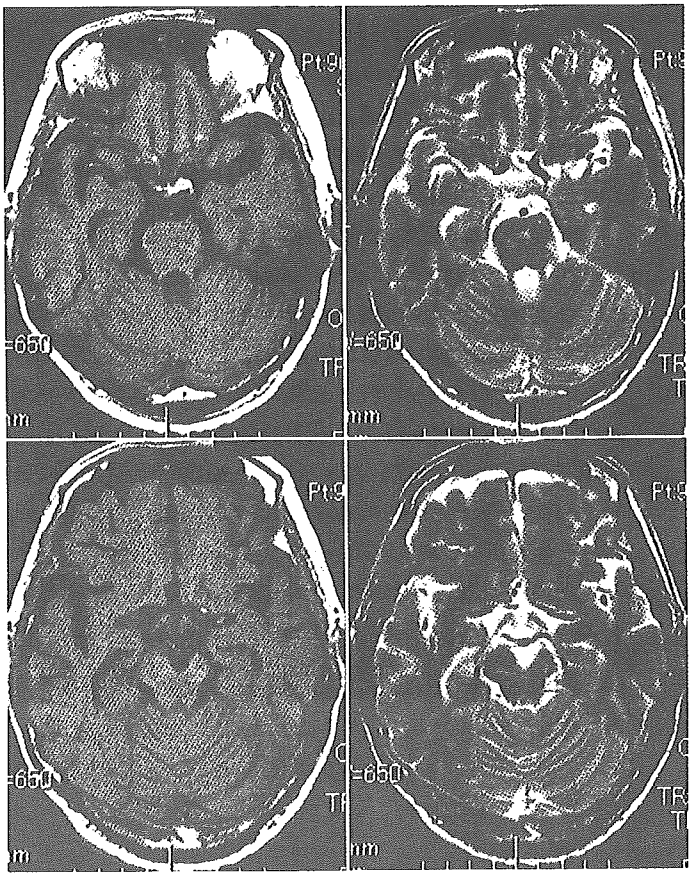

図 2　症例1，発症7年後のMRI画像
病変部位は萎縮し，T2 強調画像で高輝度を呈している．

であった．自然経過で症状が軽快し，造影効果も減弱したが，入院後 1 カ月で，炎症所見，皮膚所見が増悪，髄液所見も，810.6(L：N＝67.6：743)と増悪した．ステロイドパルス療法(メチルプレドニゾロン 1,000 mg/day 3 日間)の後，プレドニン 60 mg/day 内服開始したところ，頭痛や粘膜皮膚症状消失し，髄液所見も改善した．MRI 上は，T2 強調画像での高輝度は消失，病変部は進行性に萎縮を示した(図 2)．その後，プレドニン漸減し 20 mg/day として多幸性や興奮性も改善し退院，以後

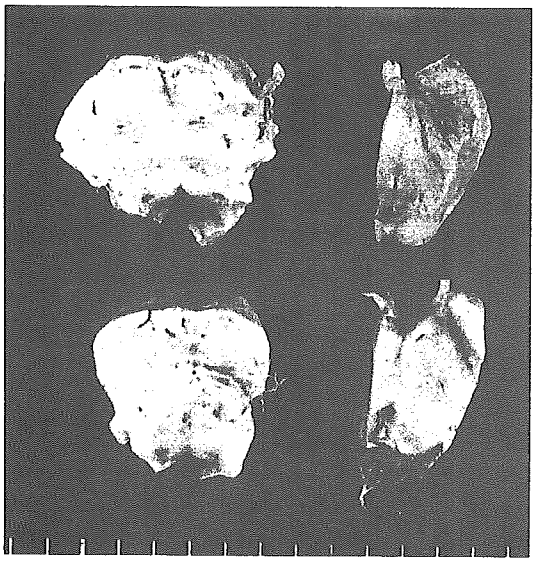

図 3　症例1，脳幹肉眼所見
MRI での病変部位は褐色沈着を示し，萎縮している．

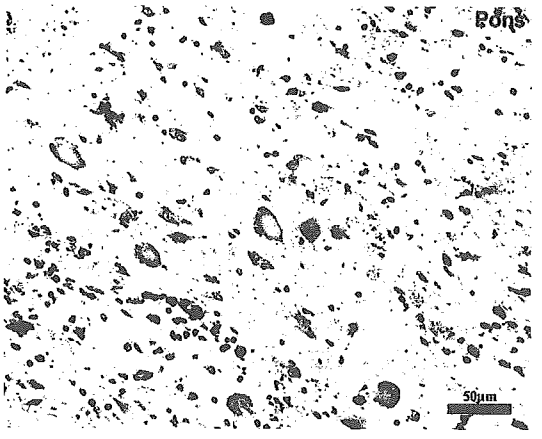

図 5　症例1，図4の病変部の拡大
Ballooned cell を多数認める．

図 4　症例1，橋でring enhanceを呈した部位の髄鞘染色
病変部位は髄鞘が消失している．

図 6　症例1，黒質(H.E.染色)
陳旧性病巣に連続し，血管周囲にリンパ球浸潤を示す，より新しい病巣の拡大を認める．ヘモジデリン沈着を認める．

外来で経過観察していた．70 歳時，胃癌および胆石のため当院外科に入院し，噴門部胃切除術および胆嚢摘出術を施行された．その後，食事がのどにつかえるという訴えを繰り返すようになり，術後吻合部狭窄に対してしばしば入院で内視鏡的拡張術を施行された．経口プレドニンは外来で漸減後中止された．術後 3 カ月ごろより食欲不振を頻回に訴え，精査目的の入院を繰り返すが，入院数日で食事摂取可能となり，タバコを吸うため勝手に院外に出てしまうことを繰り返し，そのつど退院となった．80 歳時，食欲低下で入院．衰弱著しく補液管理となるもほとんど経口摂取不能で第 24 病日死亡した．

神経病理所見[3]：死後時間 7 時間 57 分．脳重 1,095 g．肉眼的に，橋上部底部背側から黒質網状層に至る線状の褐色沈着を伴う萎縮病巣を認めた(図 3)．そのほか，左後頭極の萎縮を伴う虚血病巣，左内包前脚線状・淡蒼球・視床下核にかかる褐色沈着を伴う萎縮病巣が認められた．組織学的に，橋の病変は髄鞘が完全に消失しているかたちをとり(図 4)，同部では中心色素融解を示す神経

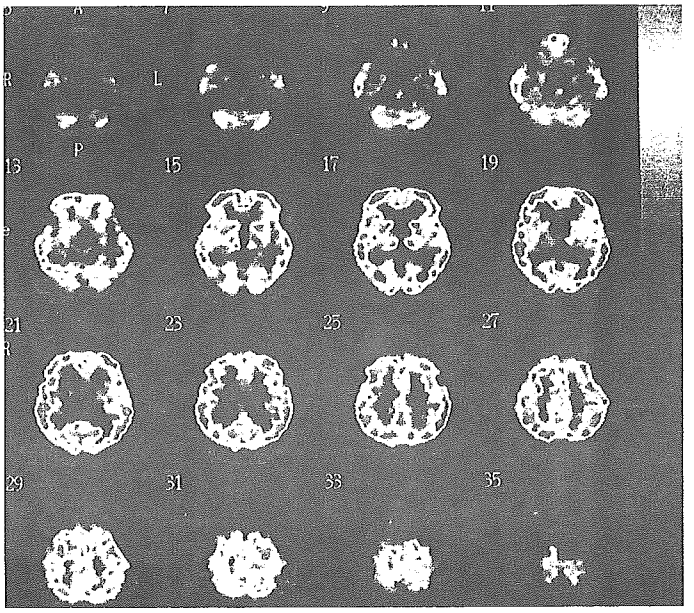

図 7　症例2，脳血流シンチグラフィ(HM-PAO)
皮質のまだら状の低下と脳幹・小脳の著明な血流低下を認める．

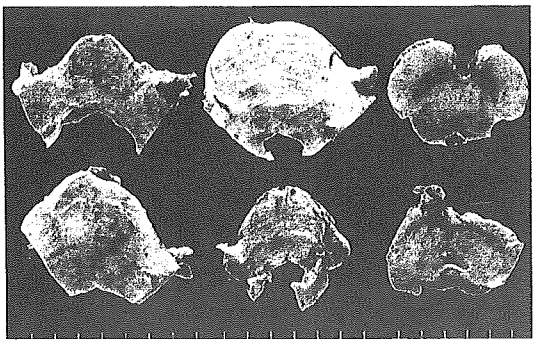

図 8　症例2，脳幹の肉眼所見
中脳と橋上部の限局性の萎縮を認める．病変部位から免れているところの萎縮は軽度である．

細胞を認めた(図 5)．髄鞘に比べ，軸索は一部保存されていた．また，グリオーシスに加え，ヘモジデリン沈着を認めた．この陳旧性病変より上に広がる形で，リンパ球の集簇を血管周囲に認め，周囲の組織の粗鬆化が観察され，より新しい変化と考えられた(図 6)．この変化は黒質網状帯より淡蒼球に至る部位に認められ，病変が拡大している経過が予想された．

2. 症例2

死亡時 40 歳男性．神経 Behçet 病に伴う脳幹脳炎の診断で，歩行障害を示したが，臨床的により

図 9　症例2，乳頭体を通る大脳冠状断割面
左海馬，右基底核・乳頭体の軟化を認める．

問題であったのは病識の欠如と亜急性進行性痴呆による介護困難であった．脳血流シンチ上は皮質

図 10　症例2，黒質(Klüver-Barrera染色)
不全軟化による髄鞘消失と血管周囲区の拡大を認める．

下痴呆のパターンであった(図 7)．副腎皮質ホルモンにほとんど反応せず，cyclophosphamide による治療中，日和見感染による敗血症により死亡した．

死後時間 2 時間 44 分で剖検．脳重 1,350 g．肉眼的に，外表所見でテント上には著変なく，脳幹の萎縮を認めた．割面で，中脳と橋上部に限局した褐色沈着と萎縮を認めた(図 8)．両側乳頭体とその周囲はやはり萎縮と褐色沈着を示した(図 9)．組織学的に，髄膜にはびまん性にリンパ球浸潤を認め，とくに脳幹・小脳部で強かった．視床では，小リンパ球の血管周囲性軽度浸潤と軽いグリオーシスの所見を認めた．中脳では組織の粗鬆化と神経細胞脱落を認め(図 10)，リンパ球浸潤を散見した．橋では下降線維が著減し，二核の神経細胞が橋核に散見された．延髄でも，局所的リンパ球浸潤と組織の粗鬆化とグリオーシスを認めた．延髄錐体は萎縮し，有髄線維脱落が著明であった．脊髄では錐体側索路・前索路の二次変性に加え，前角への軽度のリンパ球浸潤を認めた．

3．症例3

死亡時 77 歳女性．51 歳時高血圧指摘．54 歳時より気管支拡張症で左上葉切除．難治性で感染を繰り返した．68 歳時，前頸部の有痛性紅斑，下腿の紅斑と口腔内アフタ，日光過敏症より Behçet 病を疑われた．73 歳より軽度の右片麻痺と物忘れが出現し，脳血管障害を疑われたが，CT 上病変を指摘できなかった．74 歳になり，立てない，右に倒れるという症状が出現した．神経学的に，長谷川式簡易痴呆スケール 9 点，右下方視で複視，右中枢性顔面神経麻痺，深部反射が右側で亢進，四肢では麻痺・感覚障害ははっきりせず．歩行は歩幅が広く，後方転倒傾向を認めた．両側頸部血管雑音を聴取し，血管撮影を施行した．両側頸動脈の完全閉塞，右上小脳動脈血管瘤，胸部動脈・冠動脈の狭窄を認めた．眼底所見には問題なかった．76 歳，下腹部痛で卵巣癌を発症，手術的に摘出．77 歳時，咳・痰より肺・肝転移判明．尿失禁出現．狭心痛，呼吸不全進行し，死亡した．

死後時間 12 時間 20 分．脳重量 1,240 g．頭蓋内血管では内頸動脈系が細く，椎骨脳底動脈系が高度に発達．左後交通動脈・後大脳動脈分岐部に嚢状動脈瘤あり．動脈硬化は高度で，とくに椎骨脳

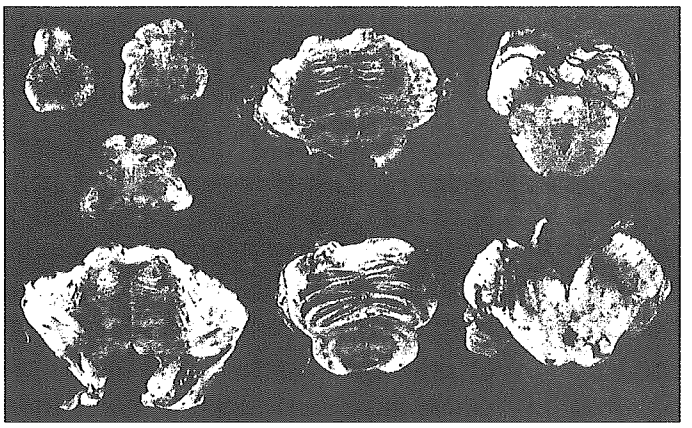

図 11　症例3，脳幹の肉眼所見
左中脳黒質腹側(矢尻)に，褐色萎縮病変を認める．

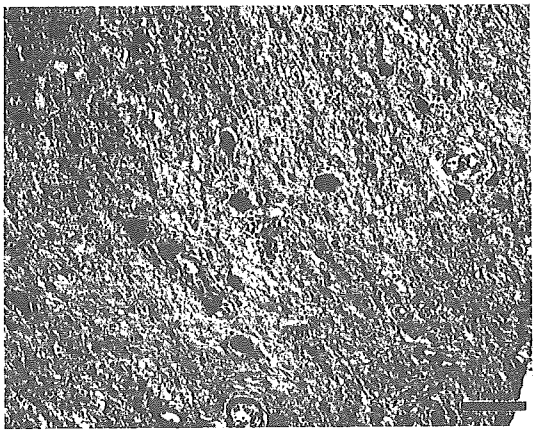

図 12　症例3，右黒質病変部
血管周囲にリンパ球浸潤を認め，背景にはグリオーシスが著明である．

底動脈系に強い．割面では左視床に空洞形成を伴う陳旧性の脳梗塞を認め，全体的に萎縮している．脳幹では，右黒質腹側に褐色沈着を伴う虚血性病巣を認める(図 11)．橋・延髄は椎骨・脳底動脈により圧迫され，縦長に変形している．組織学的に，髄膜には著変を認めない．視床においては空洞病変周囲は海綿状変化を呈しており，神経細胞が散在性に残存している．右黒質の病変部位はグリオーシスが著明で，血管周囲にリンパ球浸潤を認める(図 12)．

おわりに

自験例三例は Behçet 病の特徴を示しているが，これらの所見はかならずしも特異的でない．より特異性の高い病理所見の解明が，病因解明，治療の開発には必須と考えられる．

文献

1) 調　輝男：神経ベーチェット症候群．臨床神経病理改訂 4 版，金芳堂，1998，p.99.
2) 百瀬義雄・他：MRI 上脳幹に ring enhancement を呈した神経 Behçet 病．神経内科，**94**：190-192，1998.
3) Sakiyama, Y. et al.：Dynamic neuropathology of neuro-Behçet disease. Abstract of 82th Kanto Neuropathology Meeting, 2006.1.7. (http:/ /www.knp.gr.jp, in press)

*　　*　　*

連載　第2回

脳卒中専門医のための

神経機能解剖学

大脳白質

村山繁雄，齊藤祐子*，山之内博**，濱田　雅***
MURAYAMA Shigeo, SAITO Yuko, YAMANOUCHI Hiroshi, HAMADA Masashi
東京都老人総合研究所高齢者ブレインバンク（ゲノム神経病理），*東京都老人医療センター病理
大森赤十字病院神経内科，*東京大学大学院医学系研究科神経内科

大脳白質は膨大な容積を占めるが，構成が均一で，ヒトで最も発達しているため，機能解剖上不明の点が多い．臨床ではMRIが検査の中心であり，最近テンソル画像が伝導路の評価に開発された．病変としては，頭蓋内動脈硬化によるBinswanger型白質病変が最も重要である．血管性痴呆，パーキンソニズム，減動状態の原因となり，髄液循環障害を続発する．高血圧性心・腎病変を通常合併するため，全身評価が臨床上重要である．

Key Words
血管性痴呆，血管性パーキンソン症候群，Binswanger型白質病変，正常圧水頭症，MRI

はじめに

大脳白質は，系統発生的に，ヒトにおいて，終脳の発達が著しくなったため，膨大な領域を占めるに至った解剖学的構造であり，伝導路としてきわめて重要な役割を果たしていると考えられる．しかし，ヒトに特有であるため動物実験による病態の解明が不可能なこと，髄鞘と軸索という，比較的均一で強固な構造物により構成されるため，解析には困難がつきまとうことにより，病態が十分に明らかになっているとはいいがたい．

大脳白質の病理形態学的評価には，歴史的には，大脳全球・半球を含む大切片標本を用いることが一般的であった．しかし，大脳深部に関しては，固定が悪く，包埋剤の浸透においても問題があり，正確な評価が問題であった．大脳白質の血管支配は，穿通枝と皮質枝からなるが，大脳白質深部は，両者の境界域にあたり（図❶）[1]，虚血性病変の好発部位である．したがって，その部分の検索がむずかしいことは，大切片病理の方法論的限界である．また，近年神経病理学的検索の中心を占める，免疫組織化学染色法を適応するにあたり，大切片に対しおこなうと費用が莫大となるだけでなく，染色むらと固定むらの影響がさけられない．また，関心領域をパンチアウトで切り出し，染色する，いわゆる組織アレイ法が，大切片病理と免疫組織化学を両立させる方法としてスウェーデンより提唱されているが，固定むらの問題は解決できず，また周囲組織との関係を直接にみることができない点で，やはり限界がある．

われわれは，ヒト後天性免疫不全症（AIDS）脳症の白質病変に対し，固定後脳のMRIで検索する試みを，1999～2001年にわたり，米国ノースカロライナ大学で

図❶ 血管内バリウム注入標本の大脳前額断軟X線写真
（秋間道夫博士提供，文献1より引用）
大脳深部白質は，皮質枝からも穿通枝からも最も遠く，最末端に位置することがわかる．

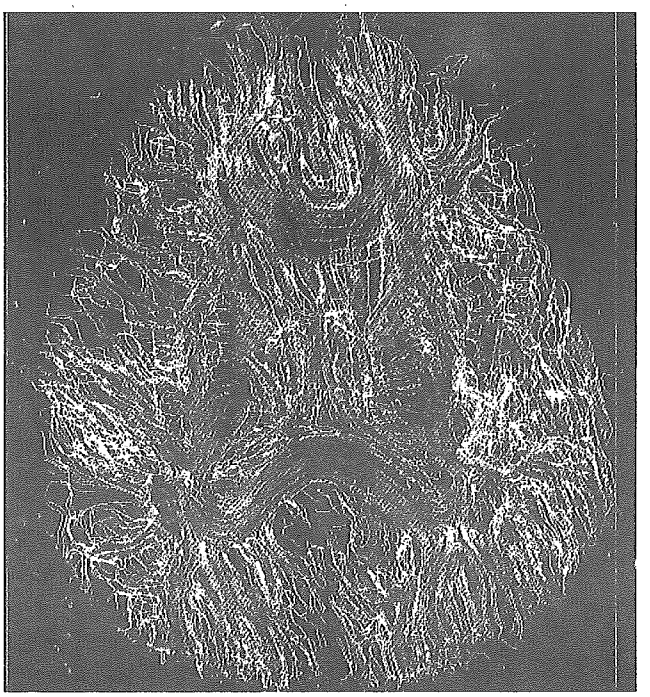

図❷ 拡散テンソル画像
拡散強調画像を利用し，伝導路を描出する．白質病変の評価に今後有用となる可能性がある（東京大学大学院医学系研究科放射線科・増谷佳孝博士開発のdTVを用いて作成した拡散テンソルトラクトグラフィー，東京大学医学部附属病院放射線科助教授・青木茂樹博士提供）．

放射線科の主導のもとにおこなった経験がある．この方法は，大脳大切片MRI染色ともよぶべきもので，生体内のMRI信号とはまったく異なるが，索変性を含む，白質病変の評価には有効であった．この方法では，固定むらが見事にT1強調画像で描出された経験がある．また，基底核がT1強調画像で高輝度を呈するなど，生体内での信号強度とは異なる点が問題であった．最近，Cambridgeのグループが，血管障害性痴呆の剖検例の評価にMRIがきわめて有用であり，生前のMRIとよく相関することを報告している．しかし，Postmortem MRIの検索においては，死亡直後にMRIを撮像しても，血流の途絶による影響がきわめて大きいことが明らかであり，異なった検索法と考えるほうが素直である．

最近，拡散テンソル画像が伝導路の検索に有用であることが示されている（図❷）[2]．この方法は，拡散強調画像を高解像度で撮ることに他ならず，現在，錐体路の部位同定，筋萎縮性側索硬化症における索変性の検出に，われわれは臨床応用している．大脳白質病変に関しては，有用性が期待される．

表❶ 東京都高齢者ブレインバンクの構成

1. 高齢者臨床神経病理リゾース	
連続剖検例（1972.5～）：7,658例（6,699脳）	
臨床・画像・病理所見	
（病歴・標本・ブロック保存）	
2. 高齢者DNAリゾース	
DNA保存例（1995.1～）：1,861例（1,517脳）	
老年病ゲノム研究の基礎資源	
3. 高齢者凍結脳リゾース	
半脳凍結保存例（2001.7～）：（417例）	
あらゆるヒト脳研究の基礎資源	

2005.3.4 現在

以下に，大脳白質の病理学的検索に関するわれわれの試みを示す．

1. 対象

東京都高齢者ブレインバンク（表❶）[3]は，1972年からの，東京都老人医療センター連続剖検例から構成されているが，神経病理専門医が全例を評価してきたこと，

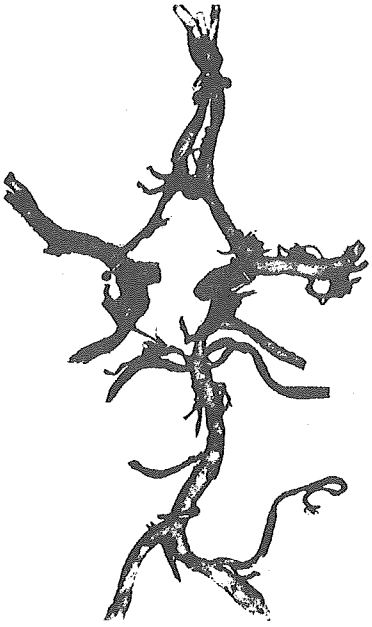

1972年5月：当施設で最初の例

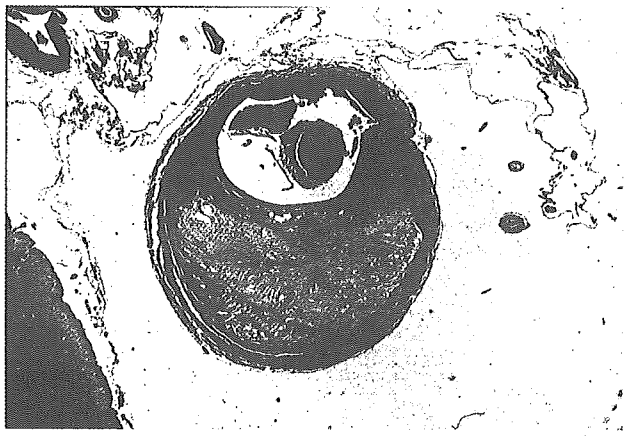

粥状硬化

図❸　血管病変の評価
Wills動脈輪を分離して評価し，必要に応じ組織学的に確認をおこなう．

表❷　頭蓋内動脈硬化指数

IntraCranial Atherosclerotic Index（ICAI）

1. Semiquantative evaluation of the grade of atherosclerosis of the intracranial arteries (Kameyama 1972)
2. Standardization by a single doctor (Dr. Yamanouchi H)

	0	1	2	3
Stenosis	0％	＜50％	50％≦＜90％	90％≦

ICAI＝summation of the grade of bilateral middle cerebral arteries and basilar artery

亀山正邦博士の開発された方法を，筆者のひとりである山之内が32年にわたりおこなっている．血管閉塞の最強部位の程度を，半定量化，両側中大脳動脈と脳底動脈におけるグレードを足し，0～9の10段階に分類している．
（小山俊一ほか，2003[4]より引用）

表❸　脳血管障害の臨床病理学的評価

臨床情報	
・脳卒中発作の有無	0, 1, 2, 3
・放射線画像	CT, MRI
	SPECT, PET

大脳白質病変は，画像所見を重視，病理対応を図る

病理データベース	
・塞栓（embolism）：	E, e
・血栓（thrombosis）：	T, t
・ラクナ梗塞（lacuna）：	L, l
・脳内出血（hemorrhage）	H, h
・くも膜下出血	SAH

臨床症状に寄与，あるいは二次変性を伴えば大文字，死戦期のものは括弧内

脳卒中発作の有無と回数，放射線画像はデジタル保存しデータベース化している．大脳白質病変は，画像所見を参考に，病理学的に対応を図っている．また心臓弁膜症に準じ，臨床症状に寄与，あるいは二次変性を伴っていれば大文字，死戦期のものは括弧内に入れて記載している．

神経内科との合同のブレインカッティングカンファレンスで，臨床・画像・病理連関が試みられてきたこと，病歴・ブロック・標本がすべて保存されており，後方視的検討が可能であることが特徴である．

2．方法

頭蓋内動脈硬化については，Wills動脈輪（図❸）について，表❷にかかげるような評価を用い，頭蓋内動脈